

## **BALL MILLED BAUXITE RESIDUE AS A REINFORCING FILLER IN PHOSPHATE-BASED INTUMESCENT SYSTEM**

*Adiat I. Arogundade<sup>1\*</sup>, Puteri S. M. B. Megat-Yusoff<sup>2</sup>, Faiz Ahmad<sup>2</sup>,  
Aamir H. Bhat<sup>2</sup>*

*<sup>1</sup>University of Abuja, PMB 117, Garki F.C.T, Nigeria.*

*<sup>2</sup>Universiti Teknologi, PETRONAS. Tronoh, 32610, Malaysia*

*Received 01.12.2017*

*Accepted 27.12.2017*

### **Abstract**

Bauxite residue (BR) is an alumina refinery waste with a global disposal problem. Of the 120 MT generated annually, only 3 MT is disposed via utilization. One of the significant challenges to sustainable utilization has been found to be the cost of processing. In this work, using ball milling, we achieved material modification of bauxite residue. Spectrometric imaging with FESEM showed the transformation from an aggregate structure to nano, platy particulates, leading to particle size homogeneity. BET analysis showed surface area was increased by 23%, while pH was reduced from 10.8 to 9.1 due to collapsing of the hydroxyl surface by the fracturing action of the ball mill. Incorporation of this into a phosphate-based fire retardant, intumescent formulation led to improved material dispersion and the formation of reinforcing heat shielding char nodules. XRD revealed the formation of ceramic metal phosphates which acted as an additional heat sink to the intumescent system, thereby reducing char oxidation and heat transfer to the substrate. Steel substrate temperature from a Bunsen burner test reduced by 33%. Therefore, ball milling can serve as a simple, low-cost processing route for the reuse of bauxite residue in intumescent composites.

**Keywords:** bauxite residue; ball milling; intumescent; reinforcing filler; ceramic phosphate.

### **Introduction**

Bauxite residue (BR) is the refinery waste from the processing of bauxite to alumina using the Bayer process. Due to the caustic hydrothermal process, untreated BR is a slurry with a pH of about 10-13 and a liquid content of 60-80%, depending on refinery practice [1]. Due to the enormous volume of generation and slurry nature, BR is commonly stored in holding ponds. To alleviate this disposal problem, a large body of work has accumulated on the reuse of BR. One of the main challenges to

---

\* Corresponding author: Adiat I. Arogundade, [adiatarogundade@gmail.com](mailto:adiatarogundade@gmail.com)

implementation of proposed applications according to *Klauber et al.* is the relatively high cost of processing and the complexity of incorporating new machinery into existing process lines [2].

In previous work, we have proposed BR as a synergistic filler in the intumescent coating (IC) [3]. Intumescent coatings are heat shielding coatings which degrade at high temperature to form an insulative heat layer [4-6]; this is an emerging technology in the fire protection of structural steels. BR contains thermally stable metal oxides, zeolitic mineral hydrates and fuel diluting carbonates which are usually employed as synergistic fillers in IC [7]. In this work simple, low-cost ball milling process was used to enhance BR property for better performance in the intumescent system. Ball milling consists of a repetitive molding and fracturing action caused by the successive compressing and impacting forces of the steel balls. This mechanical action is primarily associated with particle reduction. However, mechanochemical changes such as modification of hydroxyl surface and crystallinity have also been reported [8, 9]. Modification of the as-received BR was achieved, and the material properties were enhanced with consequent improvement in heat shielding performance. The main attraction is in the simplicity of processing and the ease of production, thus giving it high potential as a sustainable disposal outlet for bauxite residue.

## Experimental

Virotec Plc., Australia supplied the bauxite residue used in this study. The fire-retardant components for the basic formulation included expandable graphite (EG) as the carbon source, melamine (MEL) as the blowing agent and boric acid (BA) as a mineral additive. All these were purchased from Sigma-Aldrich Sdn. Bhd. Malaysia. The acid agent, ammonium polyphosphate (APP) was supplied by Clariant (Malaysia) Sdn.Bhd. The composite matrix made up of Bisphenol epoxy resin BE-188 and tetra ethylene tetraamine (ACR H-2310) as a hardener, were purchased from McGrowth Chemical Sdn.Bhd.Malaysia.

The as-received BR was dried in a muffle furnace at 105 °C for 24 hours to avoid sieve clogging. It was then sieved using an ASTM sieve with a mesh size of 65 µm. Ball milling was carried out using a roller-type ball mill from Stoneware. Milling was carried out by varying milling time from 0.25 hours to 3 hours at a constant milling speed of 300 rpm and mass to steel ball ratio of 1:8. Material characterization was done using a variable field emission scanning spectrometer to study the microstructure. Particle size distributions were compared using a nano zeta analyzer; the surface area was evaluated using the BET formula on a micromeritic surface area analyzer. Material crystallinity was obtained on an S8 Bruker-type diffractometer.

The bauxite residue intumescent coatings (BR-ICs) were prepared by incorporating ball milled (BBR) and the unmilled BR into the control formulation (BR-IC0) using high shear mixing. The mix was then applied to sandblasted, grease-free steel plates of 10x10x2 cm for the Bunsen burner test. Bunsen burner test is modeled after the ASTM E119 fire test for evaluating heat shielding efficiency of a coating on steel plates [10]. Two thermocouples were attached to the uncoated face of the IC plates while hydrocarbon fire from a butane torch was impacted on the coated face for 60 minutes. The average temperature reading for the uncoated surface was taken as a direct measure of the heat shielding efficiency of the system. The intumescent formulations are presented in Table 1. BR-IC0 represents the control formulation while BR-IC5

represents the IC formulation with 5% loading of the unmilled BR. BBR/0.25H-IC represents the formulation with BR ball milled for 0.25 hours. This naming pattern is repeated for the rest of the formulations.

*Table 1. Formulations for the intumescent coating systems (ICs).*

Specimen	COMPONENTS (g)						
	APP	BA	EG	Melamine	BR*	Epoxy	Amineer
BR-ICO	11.76	11.5	5.8	5.6	0	42.1	21
BR-IC5	11.76	11.5	5.8	5.6	5	42.1	21
BBR/0.25H-IC	11.76	11.5	5.8	5.6	5	42.1	21
BBR/0.5H-IC	11.76	11.5	5.8	5.6	5	42.1	21
BBR/3H-IC	11.76	11.5	5.8	5.6	5	42.1	21

\* where properties of BR\* changes with ball milling time from 0-3 hrs.

## Results and Discussions

The effects of ball milling on material morphology are shown in Fig. 1. Micro images from the FESEM results showed a modification of the cementitious layer from that of amorphous nano covering to small, flaky particles caused by the compressing action of the steel balls. Continuous ball milling led to fracturing and reduction of the flakes to nanoparticles.

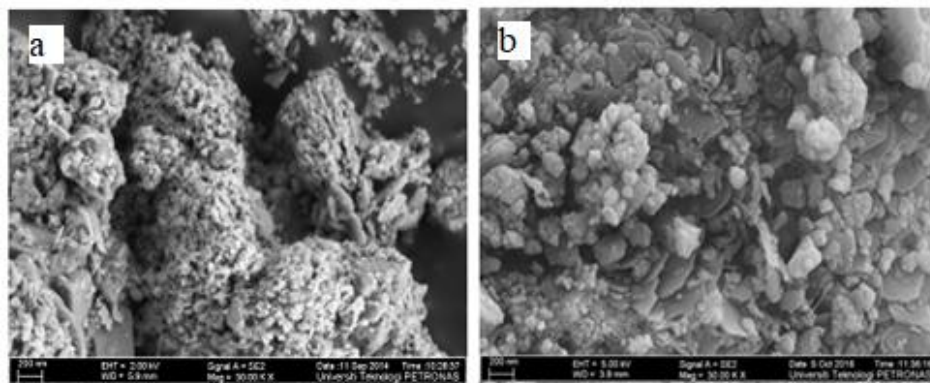


*Fig. 1. Micrographs of (a) unmodified BR and (b) BR ball milled for 0.5 hours.*

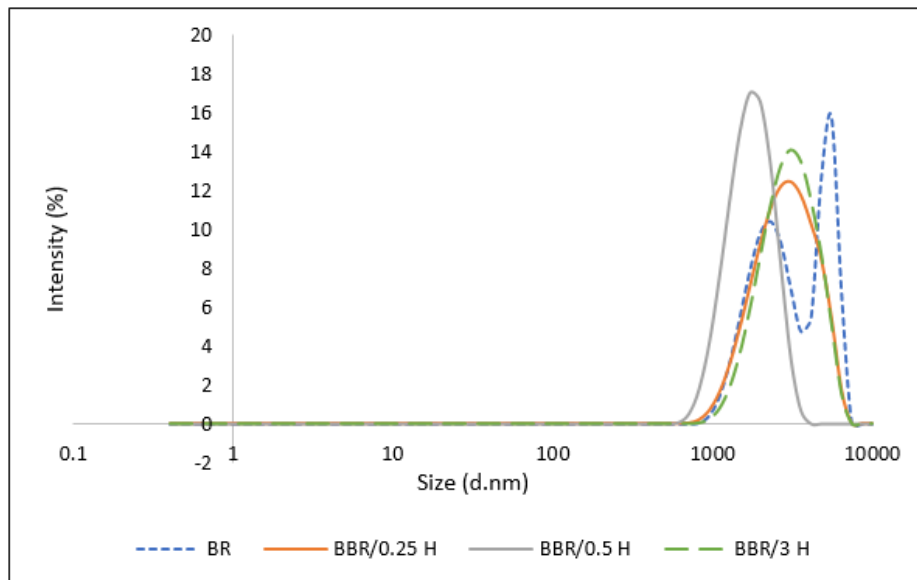


Fig. 2. Comparing particle size distribution of unmodified BR and ball milled BR at 0.25 h, 0.5 h, and 3 h.

The effect of ball milling on the particle size distribution of BR are presented in Fig. 2. Particle size analysis (PSA) of the unmilled BR showed a bimodal distribution with zeta average at 2.3  $\mu\text{m}$  and 5.6  $\mu\text{m}$ . However, ball milling at all 3 milling times reduced the PSD curves to a normal distribution indicating deaggregation of particles and their redistribution to a more homogeneous state. Zeta average shifted to 3.1  $\mu\text{m}$ , 1.7  $\mu\text{m}$  and 3.1  $\mu\text{m}$  for BR ball milled at 0.25 hour, 0.5 hour and 3 hour milling time respectively. The elimination of the finer-size particle population at 2.3  $\mu\text{m}$  zeta average agrees with the FESEM results which showed the removal of the fine cementitious layer by the molding action of the ball mill. Improved particle homogeneity would have a direct effect on BR performance in the intumescent system as homogeneity will ease particle diffusion and migration to the melt surface with subsequent improvement in barrier effect and heat shielding [11].

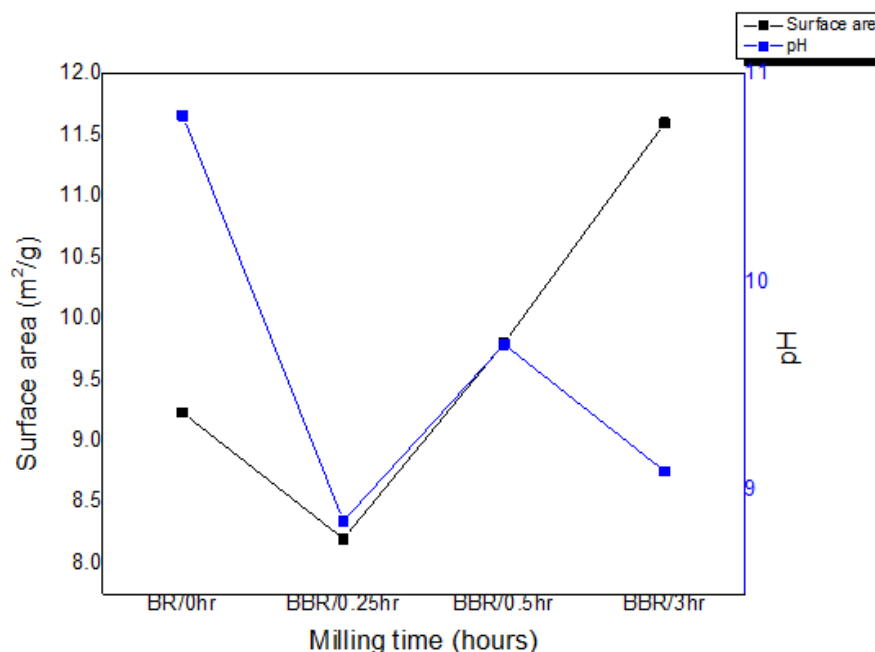


Fig. 3. Effects of ball milling on surface area and pH with increasing milling time.

Effects of ball milling on the surface area and pH of BR are illustrated in Fig. 3. The unmodified BR has a specific surface area (SSA) of 9.23 m<sup>2</sup>/g and a pH of 10.8. Initial ball milling for 0.25 hour led to a reduction of SSA to 8.2 m<sup>2</sup>/g due to compaction of the surface pores. pH was also reduced from 10.8 to 8.5 due to the collapse of the surface hydroxyl bonds by the compacting force of the ball mill. Both SSA and pH increased with milling time as the fracturing action of the ball mill revealed inner layer minerals to the material surface. SSA increased progressively with milling and was maximum at 3 hours milling due to the formation of pores and defects. On the other hand, the value of pH alternates in a reciprocating manner as hydroxide layers are repeatedly exposed and destroyed by the ball milling process. While increased surface area would improve the possibility of chemical reaction with the IC components, reduced pH inadvertently raised the affinity of the metal surface for phosphate adsorption. Both actions would expectedly contribute to the formation of a barrier layer necessary for the efficient heat shielding performance of an intumescent system. Similar effects were reported by *Tang et al.* where the surface activation of a metakaolinite filler led to improved flame retardant effect in polypropylene due to the creation of Lewis sites [12].

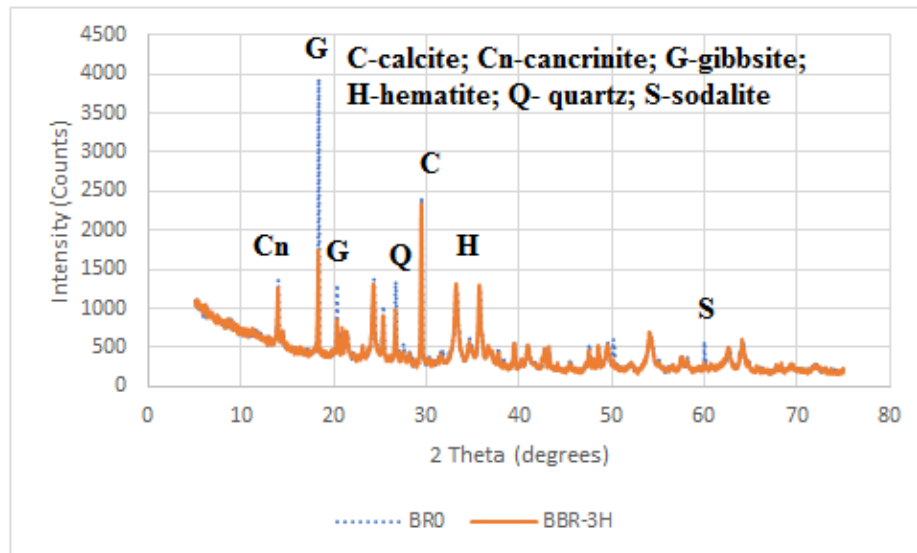


Fig. 4. XRD graphs of BR ball milled for 3 hours, and the unmodified showing reduced crystallinity due to ball milling.

The effect of ball milling on material crystallinity at 3 hours is illustrated in Fig. 4. The crystallinity of the hydroxyl minerals, most notably gibbsite is seen to be greatly reduced by the crushing action of the mill. This is due to the collapse of the O-H bond. Quartz, cancrinite, and sodalite are also affected to lesser degrees. However, hematite appeared least affected. Reduction in material crystallinity due to ball milling is a well-reported phenomenon [13, 14].

Ball milling led to a more uniform dispersion of BR in the IC system and reduced the occurrence of agglomeration. Surface mapping of the unmodified BR-IC cured matrix and the system ball milled at 3 hours BBR/3hr-IC5 are compared in Fig. 5. BR-IC showed agglomerates of phosphates and aluminates in the cured matrix, while the ball milled BR filled system showed the homogeneous dispersion of the elements.

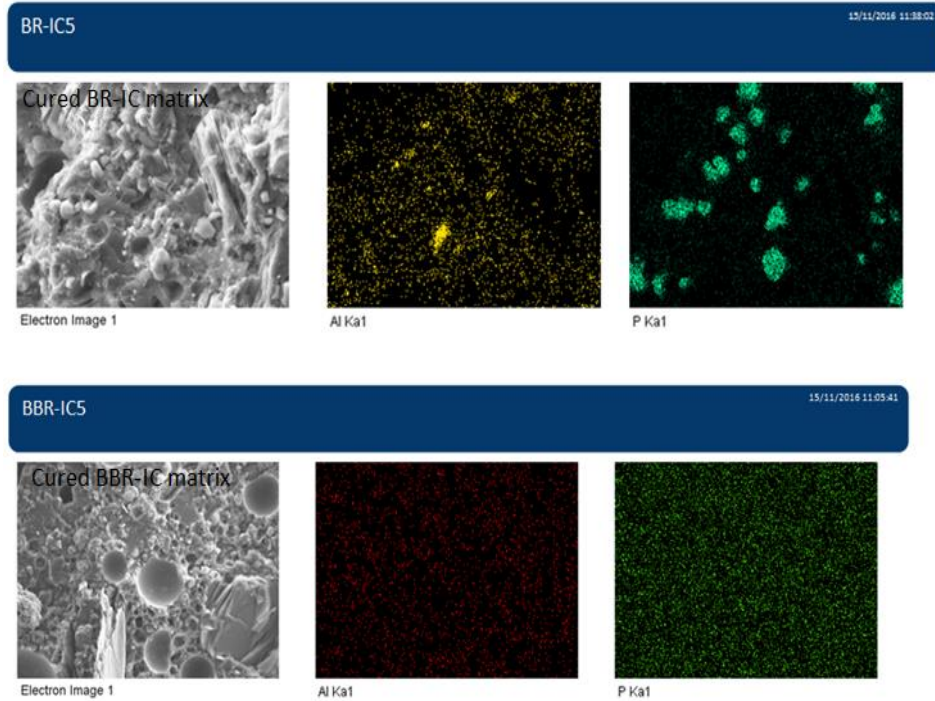


Fig. 5. Elemental mapping with EDX showing material agglomerates in unmodified system BR-IC5 and improved material dispersion in the ball milled system BBR-IC5.

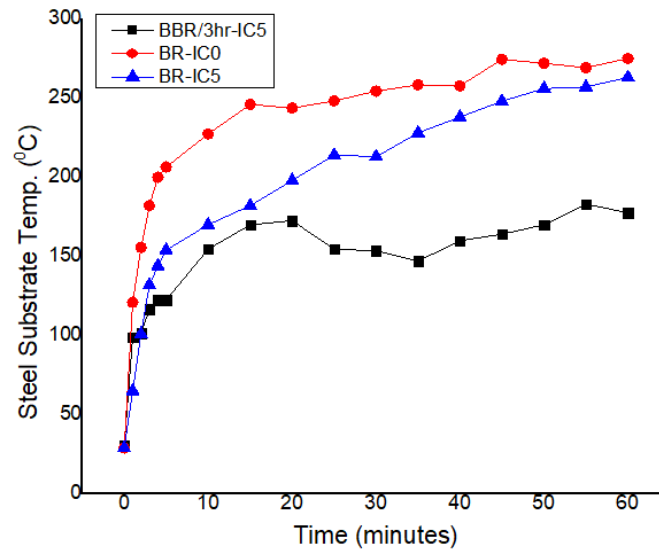


Fig. 6. Comparing heat curves of IC systems for the control, BR-IC0, the unmodified BR-IC5, and the ball milled BR-filled system, BBR/3hr-IC5.

From the heat curves of Fig. 6, a steel substrate temperature of 267 °C was recorded for the control system and 263 °C for the unmodified BR-IC5 system. On the other hand, BBR/3h-IC5 had a substrate temperature of 178 °C, with 33% in heat reduction compared to the control. This improved performance could be credited to the better dispersion of the ball milled BR in the IC matrix, the increased fuel diluting capacity and the increased chemical reactivity of the BR surface by the milling process.

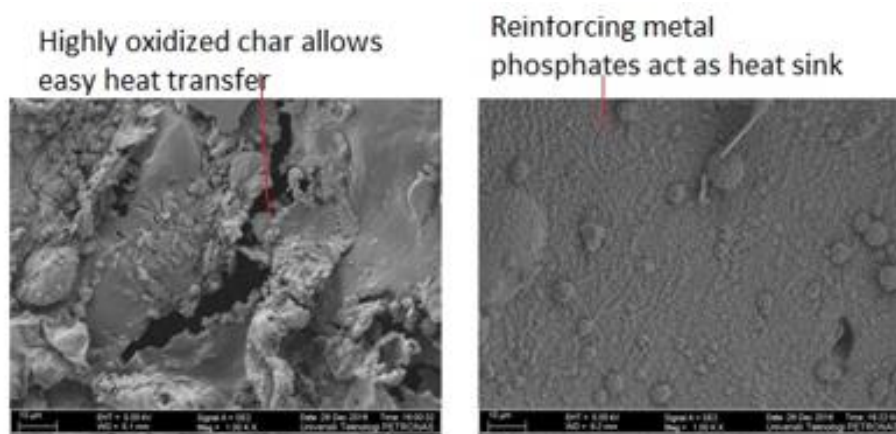


Fig. 7. Microimage of the char surface of BR-IC0 and BBR/3 h-IC5 at 1000 °C  $\pm$  100 °C.

From Fig. 7, FESEM images of the chars from the Bunsen burner test revealed the formation of char nodules which created a continuous matrix on the char surface and the inner walls and outer edges of the char cells. This proliferation of material confirmed to be metal phosphates by the XRD result of Figure 8 substantially reinforced the char structure and acted as an additional heat sink to the IC system, thereby increasing the heat shielding effect of the char.



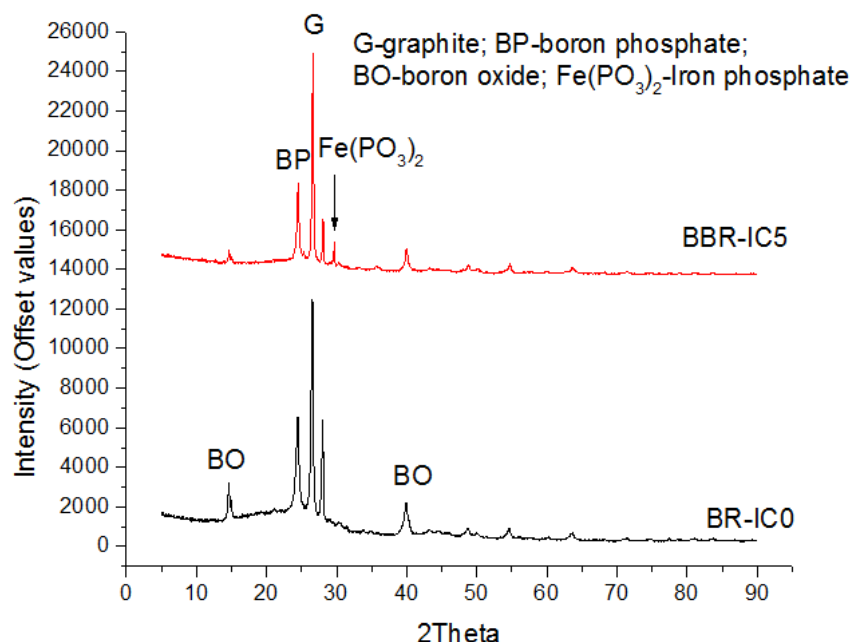


Fig. 8. Comparing XRD peaks of the chars for BR-IC0 and BBR/3 h-IC5

The characteristic peaks for the basic intumescent char are graphite (C), boron oxide (B<sub>2</sub>O<sub>3</sub>) and boron phosphate (BPO<sub>4</sub>) peaks. Boron phosphate is produced from the thermal oxidation of boron oxide and its reaction with phosphate moiety from ammonium polyphosphate. This is in agreement with earlier results reported in the literature [15]. From Fig. 8, these peaks are reproduced in the BBR-IC char. In addition to this, single peak at 29 2 $\theta$  with a d-spacing of 2.93764 Å confirmed the material accumulation in BBR-IC char as iron phosphate (FePO<sub>4</sub>).

## Conclusion

Ball milling has been employed as a simple process tool to modify and improve the properties of bauxite residue as a reinforcing filler in an ammonium polyphosphate based intumescent coating system. Particle size was homogenized from a bimodal distribution to a normal distribution, and zeta average reduced from 3.95  $\mu\text{m}$  to 1.7  $\mu\text{m}$ . Surface area increased by 23% and pH reduced from 10.8 to 9, thereby increasing BR affinity for the IC phosphates. This led to the formation of ceramic metal phosphates. The continuous formation of metal phosphates in the char matrix created additional reinforcing, heat shielding effect to the intumescent system, leading to a 33% reduction in steel substrate temperature. Thus, in this work, ball milling has been shown as a low cost, simple process route for improving the material properties of bauxite residue, particularly as a reinforcing filler in a phosphate-based intumescent system.

### Acknowledgement

The authors wish to acknowledge Universiti Teknologi, PETRONAS, Malaysia for sponsoring this research work. And one of the authors wishes to acknowledge the University of Abuja for the opportunity of Fellowship.

### References

- [1] Y. Liu, R. Naidu: Waste Manage, 34 (2014) 2662-2673.
- [2] C. Klauber, M. Gräfe, G. Power: Hydrometallurgy, 108, (2011) 11-32.
- [3] A. I. Arogundade, P. S. M. B. Megat-Yusoff, F. Ahmad, A. H. Bhat: ARPN J Eng Appl Sci, 11 (2016) 12165-12169.
- [4] J.-w. Gu, G.-c. Zhang, S.-l. Dong, Q.-y. Zhang, J. Kong: Surf Coat Technol, 201 (2007) 7835-7841.
- [5] H. Aziz, F. Ahmad, P. S. M. B. M. Yusoff, M. Zia-ul-Mustafa: MATEC Web Conf, 13 (2014) 04013.
- [6] B. Rimez, H. Rahier, M. Biesemans, S. Bourbigot, B. Van Mele: Polym Degrad Stab, 121 (2015) 321-330.
- [7] T. C. Santini: Int J Miner Process, 139 (2015) 1-10.
- [8] F. Delogu, G. Gorrasi, A. Sorrentino: Prog Mater Sci, 86 (2017) 75-126.
- [9] R. Hamzaoui, F. Muslim, S. Guessasma, A. Bennabi, J. Guillin: Powder Technol, 271 (2015) 228-237.
- [10] M. Gomez-Mares, A. Tugnoli, G. Landucci, F. Barontini, V. Cozzani: J Anal Appl Pyrolysis, 97 (2012) 99-108.
- [11] G. Marosi, A. Marton, A. Szep, I. Csontos, S. Keszei, E. Zimonyi, et al.: Polym Degrad Stab, 82 (2003) 379-385.
- [12] W. Tang, S. Zhang, J. Sun, H. Li, X. Liu, X. Gu: Thermochim Acta, 648 (2017) 1-12.
- [13] X. Yuan, S. Liu, G. Feng, Y. Liu, Y. Li, H. Lu, et al.: Korean J Chem Eng, 33 (2016) 2134-2141.
- [14] E. Leonel, E. Nassar, K. Ciuffi, M. dos Reis, P. Calefi: Cerâmica, 60 (2014) 267-272.
- [15] S. Ullah, F. Ahmad: Polym Degrad Stab, 103 (2014) 49-62.



Creative Commons License

This work is licensed under a Creative Commons Attribution 4.0 International License.